Prediction of a Container Ship Squat in Suez Canal Using CFD

Osama M. EL-Desouky [1,], Yasser El-henawy[2]*

1 Suez Canal Economic Zone Authority, Port Said, Egypt, *usama_desouki@yahoo.com*
2 Mechanical Power Engineering Department, Port-Said University, Port Said, Egypt, *dr_yasser@eng.psu.edu.eg*
* *Osama M. EL-Desouky, Email address: usama_desouki@yahoo.com*

ABSTRACT

Minor grounding or contact accidents may occur from time to time in Suez Canal. However, in March 2021, the economic ramifications of a critical grounding resounded around the world and were still felt after the Ever-Given container ship was freed from the banks. The results of a computational investigation of a ship cruising through Suez Canal are presented in this study, and hopefully can be utilized to foresee and prevent future ship's squat and bank effects throughout the determination of proper trim. The KRISO Container Ship (KCS) was picked as the example vessel for this investigation, carried out through the commercial code STAR-CCM+, and representing a comprehensive CFD analysis of such an event. The governing equations are expressed in integral form by the finite-volume based solver STAR-CCM+. The CFD investigation is performed by utilizing a Reynolds-Averaged Navier-Stokes (RANS) solver, a k-ε turbulence model and the Volume of Fluid (VOF) approach. The CFD model is validated based on the ships' experimental data. The investigation empowers shipmasters and marine pilots to comprehend the effects of squat thus avoiding ship accidents when going through Suez Canal.

Keywords: CFD, RANS, STAR-CCM+, Ship Squat

1. INTRODUCTION

Statistics indicate that around 90% of all ship accidents occur in confined waters because of the complexity and high risks to the environment involved in ship handling in ports, channels and inshore traffic zones [1]. A ship's behavior and maneuverability drastically change, as the depth of water decreases and/or when the ship is near a bank. The ever-increasing size bulk carriers and container ships face significant sinkage and trim concerns in such shallow waters, possibly resulting in "ship squatting".

Ship squat-related incidents have increased in recent years, with for example the sinking of the M/V Herald of Free Enterprise in Zeebruge's port, Belgium, in 1987, and the loss of 200 lives, resulting in millions of damages. Another incident was the 1992 grounding of the Queen Elizabeth II brought about by the flooding of tanks in the bow because of harm brought about by high squat and draft increase in the ship's fore [2]. Ship owners might be faced with expenses, for example, ship repair, pay claims for oil spillage, and dry-dock charges for ship inspection when a ship is grounded due to excessive squat.

damage to buoys, grounding and other accidents that occur to sailing ships in the Suez Canal are common, with some are caused by vessel engine failure or rudder/steering issues, while others are caused by erroneous maneuvers or poor visibility due to violent sandstorms that occasionally occur in the Canal area. Such grounding accidents, depending on their location into the one-way or two-way portions of the Canal can block it and suspend traffic, resulting in cascading economic effects reverberating around the globe.

There are various methods for modeling the squat of a ship in confined waterways: numerical, experimental, and analytical techniques. Table (1) shows a comparison between them. CFD techniques are especially useful in analyzing flow problems in resistance prediction where complex fluid flow is present. While towing tank tests provide better absolute accuracy, CFD techniques can give results that are comparable to the towing tank results at a smaller cost in money and time. Numerical strategies utilizing (CFD) methods have been

demonstrated to be prepared to precisely anticipate the sinkage, trim and resistance of marine units in shallow waters. In addition, this should be possible while representing viscous impacts just as non-direct terms [4].

Table 1. Comparison between of methods [3]

No.	Method	Advantages	Disadvantage
1	**Analytic**	- Empirical information,	- Strictly limited to basic geometries and physics - Usually limited to linear problems.
2	**Experimental**	- At first glance, most realistic	- Specialized tunnels - Severe scaling issues - Tunnel calibration - Measurements accuracy, reliability and reproducibility - Cost
3	**Computational**	- Complex physics - No scaling - Steady and unsteady	- Turbulence has to be modeled

The fast development of computational resources both in terms of advanced software and faster computers is making (CFD) methods the primary tool for ship designers in solving problems related to hydrodynamics [5].

CFD softwars such as Ansys, OpenFOAM, STAR-CCM+,...etc. are widely used , STAR-CCM+ is a general-purpose CFD code that employs a number of tools useful in ship hydrodynamics, such as Dynamic Fluid Body Interaction and a 6-DOF model, and calculates accurately the hydrodynamic forces in turbulent flows. STAR-CCM+ can be used in marine and offshore engineering applications such as wave models, motion models, fluid-structure interaction…. Etc.

Ship squat in restricted water has been studied by many researchers for example. Terziev et al. (2018) used a scale model of the DTC container ship travelling through shallow water in four channels with variable cross-sectional area and ship speeds to evaluate the sinkage, trim, and resistance of ships. They calculated the trim and squat of the DTC as it advanced through different channel geometries using (CFD), slender body theory, and several empirical methods. Elsherbiny et al. (2019) used a model of the KRISO Container Ship to conduct a number of experiments (KCS). Sinkage, trim, and overall resistance were measured to assess the KCS's performance. Elsherbiny et al. (2019a) provided a set of model tests at 1:75 scale that measured resistance, sinkage, and trim fluctuations as a function of speed, water depth, and loading conditions. This was done to investigate the range of ship trim required for safe and economical sailing in restricted water, both in terms of depth and width, and to determine the optimum trim angle for ships sailing in restricted waters in order to reduce resistance and, as a result, fuel consumption. The

majority of investigations, according to the above literature, focus on rectangular cross section canals.

In that spirit, the current study aims at predicting resistance, trim, and sinkage of a container ship (KCS) advancing through the Suez Canal with a trapezoidal cross-section by using CFD based on state-of-the-art RANS solvers. Using the proposed methodology or its conclusions, additional guidance can be provided in many forms to pilots and marine traffic controllers to make informed decisions on the direction of the vessels in order to ensure maritime safety.

In the current study, the surfaces of the ship's hull and its appendages were prepared using the CAD software Rhinoceros 3D, and were subsequently, imported and meshed into the CFD software STAR-CCM+ where the simulations were generated.

The CFD results obtained are compared to those from published experimental data for validation.

2. BACKGROUND

Sailing through channels, limited passes and other difficult passes includes some fundamental duties of the shipmaster and crew. The navigation canals used in maritime transport are the Danube – Black Sea Canal, Panama Canal, Kiel Canal, Corinth Canal and Suez Canal [6]. The Suez Canal is viewed as the shortest navigational course between East and West because of its unique geographic location. It is not only significant but essential in supporting worldwide commerce since it diminishes distance, time, fuel utilization and shipping expenses.

Suez Canal is also the world's longest canal without locks. The new Suez Canal's width varies from 200 to 210m with figure (1) showing its cross-sectional area. Ordinary ships with a draft of about 20 m can pass through it with a minimum transit speed of 16 km/h (8.6 knots), and for tanker ships is 14 km/h (7.5 knots).
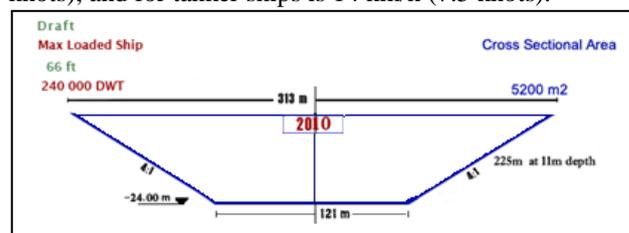

Figure 1. Cross sectional area
Source: based on [7]

3. KEEL CLEARANCE AND VERTICAL MOTIONS

A comparison of the vertical dimensions of the vessel and the canal should result in appropriate margins during the ship's transit through the access channel. An appropriate clearance between the ship's keel and the channel bottom should be maintained below the waterline. This clearance is referred to as the Under-Keel Clearance (UKC).

From figure (2) UKC$_{Gross}$ means the difference between the draft of a vessel and the declared depth of the seabed that it is traversing. While UKC$_{Net}$ will equal the sum of chart datum depth and tide and subtract both draft and squat aand other allowances from them.

The following functions should be accommodated by the (UKC):

- Contact between the keel and the bottom should be avoided.
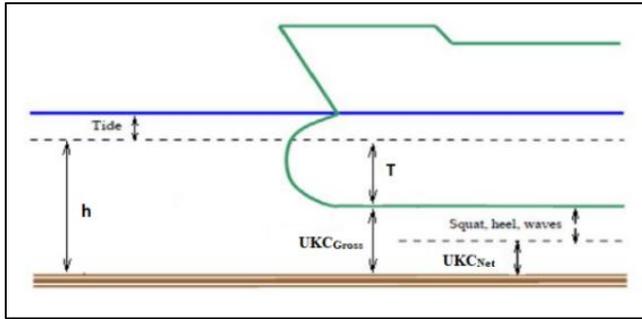- Ensure the ship's maneuverability and controllability.

Figure 2. Definition of the UKC

The clearance under the keel is determined by the following factors [8]:

- Ship factors: such as the ship's draft (fore and aft), the effect of water density on the ship's draft, in bends the heel is caused by centrifugal forces, and wave induced vertical ship motions.
- Water level factors: include effects of the tides, and weather.
- Canal bottom factors: include depth of dredging for maintenance, dredging and sedimentation.

Minimum Under Keel Clearance (UKC) can define in equation (1):

$$UKC = \frac{h - T}{T} \qquad (1)$$

Where:

h is water depth (m) and T is ship's draft (m).

The International Commission on The Reception of Large Ship (ICORELS) suggests the following values for UKC in different kinds of navigation areas [1]:

- Open sea areas: for those exposed to strong and long stern or quarter swell, where speed may be high, UKC/T should be about 0.2.
- Waiting areas: for those exposed to strong and long swell, UKC/T about 0.15.
- Channel: for sections exposed to strong and long swell, UKC/T about 0.15.
- Channel: less exposed to swell, UKC/T about 0.10.
- Maneuvering and berthing areas: for those exposed to swell, UKC/T about 0.10 to 0.15.
- Maneuvering and berthing areas: protected, UKC/T about 0.07.

4. SHIP SQUAT

Squat is caused by the ship moving through water that causes the fluid surrounding the hull to flow in the direction of the ship's bottom and sides, changing the flow pattern around the hull: where the stream rates underneath the ship accelerate, the accompanying pressure drop prompts a downward motion, changing its trim and causing an incline towards the bow or stern. When the ship is on an even keel, the overall drop in the bow or stern of the under-keel clearance relative to the depth is known as squat, as in figure (3) [9]. This phenomenon has become more important with the increasing size of tankers and bulk carriers. For ships with full forms such as oil tankers or cargo ships, the grounding due to squat occurs at the bow, and for fine form ships such as passenger ships or container vessels, grounding usually occurs at the stern.
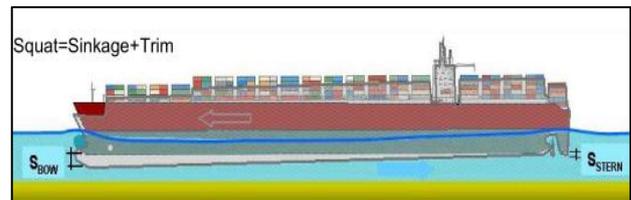

Figure 3. Ship squat

Due to the changing pressure field around the ship at speed, squat can occur even in deep water, but in shallow water, it increases and becomes more significant.

A blockage effect happens in any confined waterway when the ship's sectional area exceeds a particular proportion of the channel's cross section. For narrow channels, a blockage factor has been defined in equation (2)[6]:

$$Blockage\ factor, (S) = \frac{Ship\ Draft \times Breadth}{Canal\ Draft \times Breadth} \qquad (2)$$

The maximum squat (δmax) formula is determined by equation (3)[6]:

$$\delta_{max} = \frac{C_B \times S^{0.81} \times V_K{}^{2.08}}{20} \quad (m) \qquad (3)$$

Where:

C$_B$ is block coefficient and V$_K$ is forward speed(m/s).

Signs that a ship has entered shallow waters are [10]:

- The vessel turns out to be progressively harder to maneuver.
- Bow wave increases.
- The ship may start to vibrate.
- Rolling, pitching, and heaving actions reduces.

Squat magnitude is influenced by a number of factors [9]:

- The forward speed (V_K) which is the most essential factor, since ship squat varies directly as $(V_K)^2$.

- The block coefficient (C_B)) with the squat varying in direct proportion to the (C_B).

There are other factors which have an effect on the squat such as draft/ water ratio, propeller speed, length / breadth ratio, and initial trim.

5. SHIP RESISTANCE

The total resistance (R_T)of a vessel at a certain velocity is defined as, "the fluid force acting on the vessel in such a way as to oppose its motion" and is "equal to the component of the fluid forces acting parallel to the direction of motion of the ship". The total resistance coefficient (C_T) is a dimensionless quantity defined as in equation (4) or (5):

$$C_T = \frac{R_T}{0.5 \times \rho \times V_k^2 \times A_s} \qquad (4)$$

Where:

ρ is fluid density (kg/m^3) and A_S is wetted area (m^2).

$$C_T = C_F + C_R \qquad (5)$$

Where:

C_F is friction resistance coefficient and C_R is residual resistance coefficient.

The coefficient of friction resistance (C_F) depends on Reynolds number (R_n) and is assumed to be independent from the coefficient of residual resistance. Which can be broken down into a coefficient of wave resistance (C_W) and coefficient of viscous pressure resistance (C_{VP}), resulting in equation (6):

$$C_T = C_F + C_{VP} + C_W \qquad (6)$$

The definition of form-factor k was proposed in the context of the resistance check technique followed through the International Towing Tank Conference (ITTC) in 1978, primarily based totally on assumptions: invariance between the model and the full scale ship and invariance with relating to the Froude number (F_r) Working in this context, it is able to be written as in equation (7):

$$C_{VP} = kC_F \qquad (7)$$

The total resistance coefficient can be defined as in equation (8):

$$C_T = (1 + k)C_F + C_W \qquad (8)$$

6. COMPUTATIONAL METHOD

Nowadays, with the rapid development of computer technique and CFD methods, numerical prediction of the hydrodynamic forces has become possible. Ship maneuvering predictions by solving unsteady Reynolds-averaged Navier Stokes (RANS) equations have been presented in SIMMAN workshops (2008 and 2014) for CFD validation analysis. The RANS solver software used to carry out all the calculations in this study is STAR-CCM+ version 14.02.010-R8 [11], chosen because it contains a six-degree of freedom motion solver as well as a robust built-in automated mesh generator.

By assuming an equal Froude depth number between model and full-scale cases, the Froude depth number equation shown below can be manipulated to determine the model scale speed as shown in equations (9) & (10).

$$F_r = \frac{V}{\sqrt{gL}} \qquad (9)$$

$$V_M = \frac{V_S}{\sqrt{\beta}} \qquad (10)$$

Where:

g is gravity acceleration (m/s^2), L is ship length (m) ,V_S is ship speed (m/s), V_M is model speed (m/s) and β is factor scale.

The following assumptions were used in modeling:
1. Incompressible fluid.
2. Linear motion with constant speed.
3. Calm water conditions (the effect of the wind is not considered).
4. The ship is considered on even keel without the influence of the propeller.
5. The surface of the hull is perfectly fine.
6. Straight bottom without natural disturbances.
7. The vessel is free to trim and sink.
8. The hull mass is constant.
9. Four model scale speeds: 0.693 ,0.789,0.887, and 0.988 m/s or (1.3,1.5,1.73and 1.9) knots.
10. The flow around the hull is symmetrical about the centerline, only starboard half of the model was used to reduce the computational time.

Figure (4) shows the workflow of the STAR-CCM+ software when numerically solving a given CFD problem.
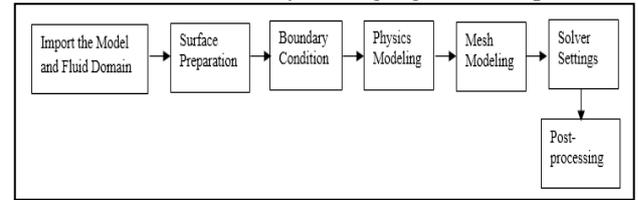

Figure 4. Workflow overview in STAR-CCM+
Source: based on [11]

6.1. Governing Equations

The governing equations of any fluid stream are the momentum, conservation of mass and energy written in integral or partial differential from. For incompressible flows, the momentum and continuity equations may be written in tensor form and Cartesian coordinates as follows (11-13) [12]:

$$\frac{\partial(\rho \bar{u}_i)}{\partial x_i} = 0 \qquad (11)$$

$$\frac{\partial(\rho \bar{u}_i)}{\partial t} + \frac{\partial}{\partial x_j}\left(\rho \bar{u}_i \bar{u}_j + \rho \overline{\acute{u}_i \acute{u}_j}\right) = -\frac{\partial \bar{p}}{\partial x_i} + \frac{\partial \bar{\tau}_{ij}}{\partial x_j} \quad (i, j = 1,2,3..) \qquad (12)$$

Where:

$\bar{u}_i$ is u, v, w the velocity components of the flow in the (x, y, z) coordinate directions(m/s), $\bar{p}$ is mean pressure (Pa) and $\bar{\tau}_{ij}$ is stress tensor.

Where $(\bar{\tau}_{ij})$ is determined by equation (13):

$$\bar{\tau}_{ij} = \mu \left(\frac{\partial \bar{u}_i}{\partial x_j} + \frac{\partial \bar{u}_j}{\partial x_i} \right) \tag{13}$$

Instantaneous velocity and pressure fields are divided into a mean value and a fluctuating component using the RANS equations.

6.2. Ship Particulars

The ship used for this study is the KCS developed by the Korean Research Institute Ships and Ocean Engineering. To reduce computational complexity, time and effort, the simulation is performed in model scale with a scale factor (β).

The main dimensions of the ship and model where all values refer to the origin located at (AP/CL/BL) are given in table (2) and in figure (5) the KCS is represented by solid lines.
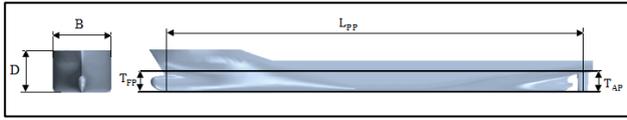

Figure 5. Body planes and side view of the KCS
Source: based on [13]

Table 2. Main dimensions of the ship and the model [13]

No.	Parameters	Units	Ship	Model
1	β		-	31.6
2	L_{PP}	m	230	7.2786
3	B	m	32.2	1.0190
4	D	m	19	0.6013
5	T_{FP}/T_{AP}	m	10.8	0.34
6	C_B	-	0.651	0.651
7	Displacement	m^3	52030	1.649
8	KG	m	7.28	0.23
9	LCG	m	111.6	3.532
10	k_{XX}	m	12.88	0.4076
11	k_{YY}	m	57.5	1.81965
12	A_S	m^2	9530	9.55275

6.3. Coordinates system

The ship moves according to two sets of coordinates, the earth fixed (O, X, Y, Z) and the body fixed (O, X1, Y1, Z1) characterized by the Cartesian coordinate system as in figure (6) Firstly, In the earth-fixed coordinate system (O, X, Y, Z), the stream field was solved, and the excitation hydrodynamic forces acting on the ship hull were computed. Secondly, the hydrodynamic forces were converted to a body coordinates system (O, X1, Y1, Z1) which was situated at the center of mass of the body. The coordinate system is characterized by the positive X- axis facing towards the bow, the positive Y-axis towards the portside and the positive Z-axis upwards. The vessel's axis is situated along the X-axis with the bow situated at

X = Lpp and the stern at X = 0. The actual water surface is at 0.34 m above the keel and the X-Y plane is parallel to the calm water surface, Z = 0.
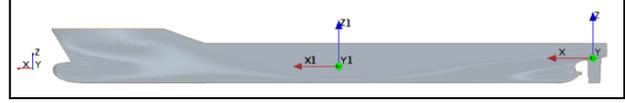

Figure 6. Hull geometry with coordinate system

6.4. Flow Region and Boundary Conditions

The domain of the simulation is the spatial region in which the simulation takes place, its shape being a trapezoid built based on the (ITTC)'s recommendation to avoid flow reflections [14].

In this study, the computational domain was selected as follows:

- The inlet boundary is defined as a velocity inlet (V_M) equal to model speed and positioned at 1.5 Lpp upstream of the forward perpendicular.
- The top boundary is defined as a velocity inlet and placed at 0.5 Lpp from the water surface level.
- The outlet boundary is located at 2 Lpp downstream of the aft perpendicular and is defined to maintain the hydrostatic pressure.
- The bottom boundary is defined as a velocity inlet and located according to Suez Canal water depth; while the Side1 boundary is defined as a velocity inlet and placed according to Suez Canal side bank distance.
- Finally, due to symmetry conditions, the Side2 boundary is located as a symmetry plane and the KCS model is defined as a wall. The general view of the computational domain is shown in figure (7).
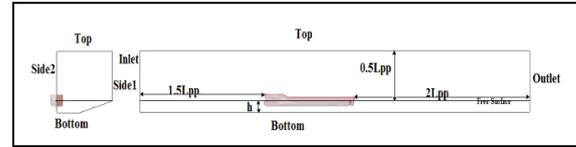

Figure 7. Boundary names of fluid domain

6.5. Physics Modeling

The physicals models used in the CFD simulations are briefly described in the following.

6.5.1. Flow Type

One aspect that will complicate the analysis of flow problems is that flows are not always stable; in fact, all flow problems will become unstable when a particular Reynolds number is reached within the flow, which will be calculated as in equation (14).

$$R_n = \frac{V \times L \times \rho}{\mu} \tag{14}$$

Where:

μ is dynamic viscosity (Pa.s).

6.5.2. Turbulence Model

The choice of a turbulence model impacts the hydrodynamic estimation. There are diverse turbulence models generally applied in engineering estimations: standard k-ε, RNG k-ε, standard k-ω, and SST k-ω. The turbulence model utilized in this study was the k-ε two-layer model with two-layer all y+ wall treatment; since it has been broadly utilized in comparative examinations to guarantee precise portrayal of ship movements [4].

The k-ε turbulence model is utilized to display the Reynolds stress tensor as well as the turbulence kinetic energy and dissipation of that energy, which adjusts the estimation of the viscous stress tensor by using the turbulent eddy viscosity(μ_t) as shown in (15)[16]:

$$\mu_t = C_\mu \frac{\rho K^2}{\varepsilon} \qquad (15)$$

Where:

ε is turbulence dissipation rate (m^2/s^3) and K is turbulent kinetic energy (m^2/s^2).

The (C_μ) is a constant equal to 0.09. the (k) and (ε) are computed locally from the transport equations of (16) and (17).

$$\frac{\partial(\rho k)}{\partial t} + \nabla \cdot \left(\rho k \overline{U}\right) = \nabla \cdot \left[(\mu + \frac{\mu_t}{\sigma_k})\nabla k\right] + P_k - \rho\varepsilon \qquad (16)$$

$$\frac{\partial(\rho\varepsilon)}{\partial t} + \nabla \cdot \left(\rho\varepsilon \overline{U}\right) = \nabla \cdot \left[(\mu + \frac{\mu_t}{\sigma_k})\nabla\varepsilon\right] + \frac{\varepsilon}{k}(C_{Z1} P_k - C_{z2} \rho\varepsilon) \qquad (17)$$

Where (P_K) is the production term and defined in equation (18)

$$P_k = \mu_t\nabla\overline{U}\cdot\left(\nabla\overline{U} + \nabla\overline{U^T}\right) - \frac{2}{3}\nabla \cdot \overline{U}[3\,\mu_t\nabla\cdot\overline{U} + \rho k] \qquad (18)$$

6.5.3. The Implicit Unsteady Model

Explicit methods require higher memory because of the moderately bigger fluid domain requested by the stream physics science of ship hydrodynamic issues. Along these lines, an implicit method is picked for a mathematical solution. In an explicit method, The Courant number (CFL) is a useful method of determining the time step, a (CFL) conditions must be respected for the stability of the method and is defined by equation (19):

$$CFL = \frac{U_O\,\Delta t}{\Delta x} \leq 1 \qquad (19)$$

The flow properties, rather than the Courant number, are frequently used to calculate the time step (Δt)in implicit unsteady simulations. An alternative method for time-step selection, proposed by the ITTC (2011) recommends that for resistance predictions, (Δt) is calculated as shown in equation (20)[14]:

$$\Delta t = \frac{0.005{\sim}0.01 L}{V} \qquad (20)$$

In the current simulations, the mesh remains constant for all speeds, while the time step is changed by the previously mentioned equation.

6.5.4. Volume of Fluid

The Volume of Fluid technique (VOF) is used to capture the free surface, developing the extra transport equation solved for the volume fraction as shown in equation (21):

$$\frac{\partial(\alpha)}{\partial x_t} + \nabla(\alpha\bar{u}_i) = 0 \qquad (21)$$

In the (VOF) method, the location is captured implicitly by determining the boundary between water and air within the computational domain. wherein the volume fraction of the phase in a computational cell (α) is zero for air, and 1 for water, and the sharp gradient around the value of 0.5 refers to the free surface, as indicated in figure (8).
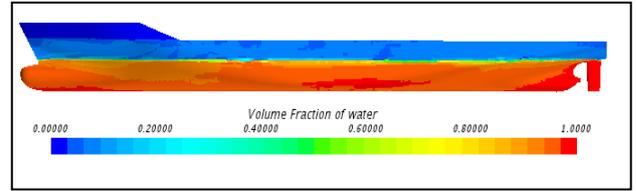

Figure 8. Free surface representation

6.5.5. Eulerian Multiphase

The Eulerian multiphase model is needed to make and manage the two Eulerian phases of the free surface simulations, each of which represents a unique physical substance. For these simulations, the two phases are salt water and air, with constant density and dynamic viscosity as defined in table (2)

6.5.6. Dynamic Fluid-Body Interaction Module

STAR-CCM+ gives a Dynamic Fluid-Body Interaction (DFBI) module. DFBI can model the motion of rigid bodies with six degrees of freedom within the fluid system. The DFBI module enables the RANS solver to determine the hydrodynamic forces acting on the vessel.

6.5.7. Initial Conditions

Initial conditions values for this study are assumed as in table (3).

Table 3. Summary of initial conditions

No.	Parameter	Unit	Value			
1	V_m	m/s	0.9886	0.887	0.789	0.693
2	R_n		6.1 ×10^{+6}	5.5 ×10^{+6}	4.9 ×10^{+6}	4.3 ×10^{+6}
3	Δt	s	0.026	0.0287	0.0322	0.0367
4	**Physical time**	s	100			
5	**Iterations per time step**		5			
6	**I**		0.01			
7	**TVR**		10			
8	$\rho_{Salt\,Water}$	kg/m^3	1025			
9	ρ_{Air}	kg/m^3	1.184			
10	$\mu_{Salt\,Water}$	Pa-s	1.21 ×10^{-3}			
11	μ_{Air}	Pa-s	1.855 ×10^{-5}			

6.6. Grid Generation

The meshing process of this study involved the following steps:

1. The ship hull and trapezoid block were modeled by using software Rhinoceros 3D. Where the block is around the ship hull that would later become the fluid domain of the volume mesh representing the water and air surrounding of the hull.
2. The ship hull surface was subtracted from the block. The simulation proceeded with the outcome of this subtraction, the subtracted block.
3. The meshing of the subtracted block was conducted using mesh generator in STAR-CCM+.
4. By using diagnostic check on the mesh in STAR-CCM+ to assess the validity of the surface and repair any errors found. This is a necessary step before starting the simulation.

The computational domain (the subtracted block) is meshing by using the following meshing tools:
1. Isotropic trimmer.
2. Surface remesher.
3. Prism layer mesher.
4. Volumetric controls.

The surface remesher improves the quality of a surface to provide a better volume mesh, while the isotropic trimmer is employed to generate a high-quality grid for complicated mesh generating problems; where the isotropic trimmer means that the elements are equally re-meshed along (x, y, z) directions. Surface remesher and isotropic trimmer options were chosen for the hull vicinity.

The prism layer mesh was utilized to generate orthogonal prismatic cells next to the ship hull to capture the velocity gradient and the boundary layer.

Volumetric controls have been used to refine the grid around the hull and the free surface, which are critical zones with complex behavior.

This is done by creating the following blocks around the hull as shown in figure (9):
1. Free surface 1 block.
2. Free surface 2 block.
3. Free surface 3 block.
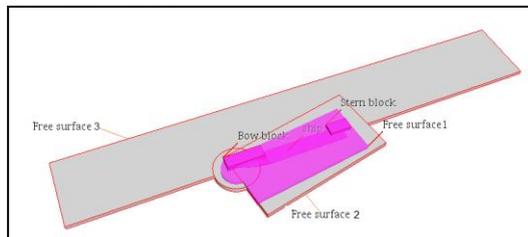4. Bow block.
5. Stern block

Figure 9. Multiple blocks for improving mesh resolutions around hull

In this study, the mesh was successfully refined as follows: coarse, medium, and fine with a refinement ratio of √2 [15]. where the cell base size is defined as a relative value for all mesh parameters, except in the case of the prismatic layers mesher, where the prism layer thickness is defined as an absolute value and the maximum number of layers was 6. The meshing details for the KSC model are given in table (4). Figure (10)

indicates the coarse, medium and fine meshes around the ship respectively and the refinements at critical zones.

Table 4. Mesh sizes in different parts

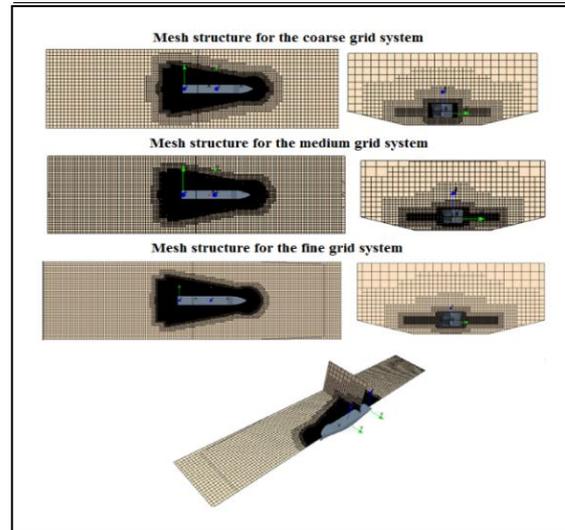| No.	Block Name	% of Base size
1	Background region	50 %
2	Free surface 1 block	25%
3	Free surface 2 block	40%
4	Free surface 3 block	200%
5	Bow block	12.5%
6	Stern block	12.5%

Figure 10. Mesh structure for the three grid systems in the fluid domain

6.6.1. Grid Independent Study

For the current study, a grid independent study of the KCS model was conducted to assess the proper total number of cells meshing for the whole simulations. The results of the grid independence study are summarized in table (5) where the number of cells and the experimental and computed total resistance coefficient at speed of 0.887 m/s for three different meshes are presented.

Table 5. Comparison of the total resistance coefficient at speed 0.887 m/s

		CFD			Exp [17]
	Unit	Coarse	Medium	Fine	
Base size	m	0.2	0.141	0.1	
Number of cells	millions	0.9	1.5	2.4	
C_{TM}	-	5.47×10^{-3}	4.2×10^{-3}	3.75×10^{-3}	3.7×10^{-3}
Difference $\left[\dfrac{\text{CFD-EXP}}{\text{EXP}}\right] \times 100$	%	47.8	13.5	1.3	

From table (5), it is evident that as the number of cells increases, the coefficient of total resistance decreases. the difference between CFD and the experimental result

38

obtained with the fine mesh is about 1.3 %; and it was concluded that the fine mesh is the most appropriate and provides good results at a reasonable computational cost. Therefore, the fine mesh was used for this study to predict the trim, resistance, and squat of the KCS model at four speeds.

7. RESULTS AND DISCUSSIONS

The simulation results obtained during this study will be described in this section; where the ship model resistance, squat and trim were calculated at four speeds. The simulations are run on the STAR-CCM+ commercial CFD software. For all simulations a segregated flow solver technique is utilized. The Realizable Two-Layer k-e turbulence model is used in an unstable RANS technique.

The calm water is simulated by utilizing a flat wave and the free surface is simulated by utilizing the (VOF) solver. To study the trim and sinkage of the KCS model, a Dynamic Fluid Body Interaction (DFBI) solver was utilized, where the two degrees of freedom of the sinkage and trim were considered in the estimation. The vessel has free rotation around the Y-axis (trim) and movement along the Z-axis sinkage; where negative sinkage indicates downwards directions from the free surface and positive trim indicates trim by bow.

The predicted sinkage, trim, and total resistance coefficient values of the KCS model using the (CFD) method will be compared to the experimental fluid dynamics (EFD) data to validate this study. In order to investigate ship squat, trim and resistance characteristics when travelling through the Suez Canal, a series of experimental tests on a KCS model were conducted in this (EFD) at the depth Froude numbers were varied from 0.1 to 0.7, and the H/T values were varied from 1.78 to 2.5. In this study, the (CFD) and (EFD) outputs will be compared at various depth Froude numbers from 0.25 to 0.36 and at a H/T ratio of 2.2.

The outcomes of (CFD) and (EFD) are displayed in this section. Suez Canal's full-scale simulation option ranges from 7 to 11 knots, translating to depth Froude numbers between 0.25 and 0.36. The Suez Canal's 7 knot maximum operational speed is the reason behind this decision [7].

In the current study, higher speeds up to 11 knots were chosen to demonstrate to ship masters and marine pilots what would happen to the ship's squat and trim if its speed increased owing to technical problems. the sinkage and trim values for the Suez Canal (CFD) and (EFD) are shown in figures (11) and (12). Figure (11), which plots sinkage changes versus depth Froude number, makes evident that there aren't many variances in sinkage between (CFD) and (EFD). Figure (12) presents trim angle variations against depth Froude numbers. The difference between (CFD) and (EFD) trim values are small.
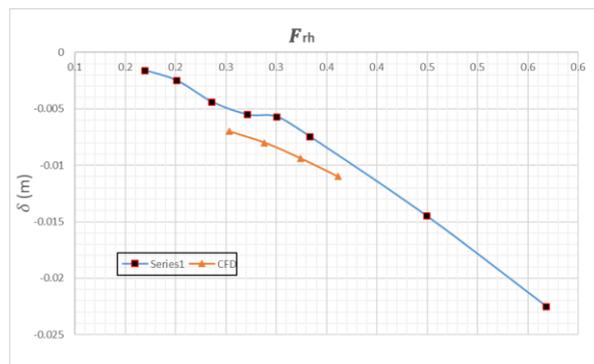

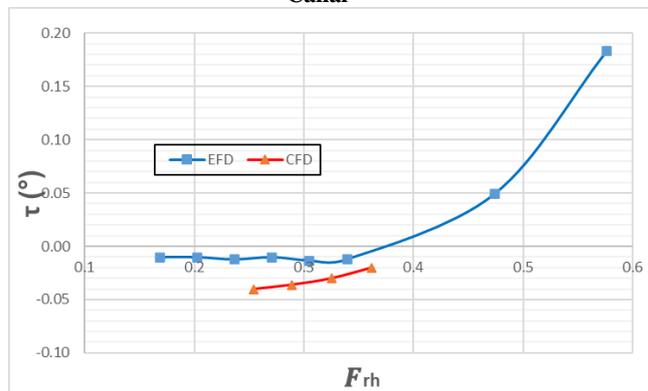**Figure 11. CFD and EFD comparison of sinkage in the Suez Canal**

Figure 12. CFD and EFD comparison of trim angle in the Suez Canal

Figure (13) shows the total resistance coefficient values computed via (CFD) and (EFD) and displays total resistance coefficient variations versus depth Froude number at a H/T ratio of 2.2.

As can be seen from this figure the total resistance coefficient values in (CFD) method decreases with increase depth Froude numbers from (0.25 to 0.36) and the total resistance coefficient increases rapidly as (F_{rh}) becomes larger in (EFD) data. The difference between (CFD) and (EFD) of total resistance coefficient values are small. Figures (11), (12), and (13), show how well the predictions of sinkage, trim, and total resistance coefficient from (CFD) method agrees well with (EFD) results.
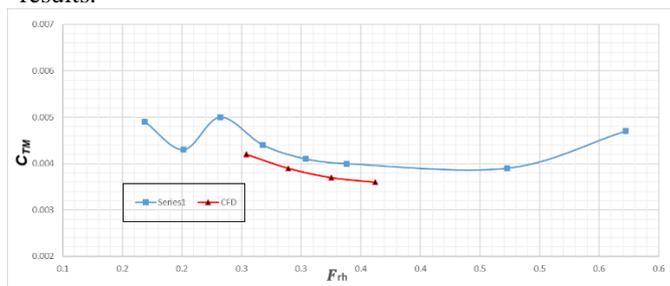

Figure 13. CFD and EFD comparison of total resistance in the Suez Canal

Ship masters and marine pilots may use figure (14) that shows the varieties of the KCS sinkage (8) and trim angle (τ) at four speeds to give them rapid thinking

about ship hydrodynamics during sailing in the Suez Canal instead of using mathematical equations.

For example, when they decide to sail their ship through the Suez Canal at a ship speed of 0.887 m/s, by using figure (14) they find the sinkage (δ) is 0.0094 m under of the free surface level and the trim angle (τ) is 0.03 by stern, and with an increase in ship speed, the trim degree changes from stern to bow trim Therefore, the figure(14) gives a simple and easy technique for shipmasters and marine pilots to know the ship's behaviour during sailing and estimate the sinkage (δ)and trim angle (τ) for container ships to reduce the time consumed in complicated calculations.
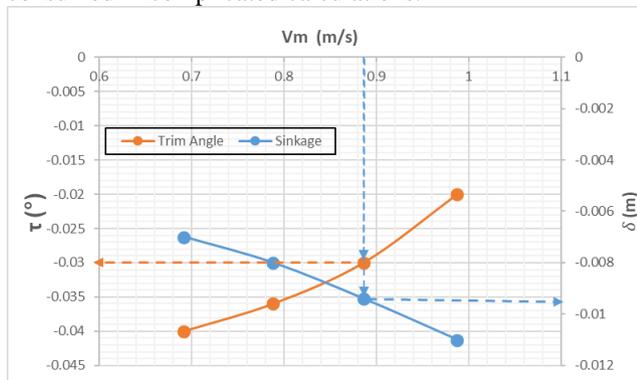

Figure 14. Sinkage and trim angle curves

As seen in figure (15) with the speed up, the ship's body sinks during voyaging, which is joined by the phenomenon of trimming by the bow. The level of sinking of the ship's body increments with the speeding up and the level of trimming by the bow of the hull diminishes. As per the above investigation, there are more vortices in the stern, which makes the stern pressure decline. Consequently, the augmentation of the return stream speed in the stern of the ship is bigger than that in the bow and the stern sinks to a greater degree than the bow; which brings about a decrease in the degree of trimming by the bow, figure (15) shows the pressure distribution around the ship at different speeds.
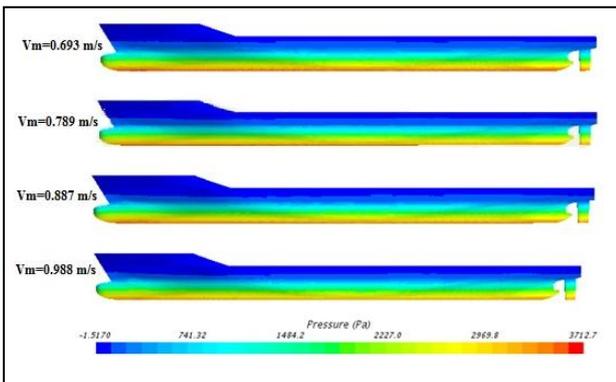

Figure 15. Distribution of pressure throughout the ship

8. CONCLUSION AND FUTURE WORK RECOMMENDATIONS

This paper explores the ship squat phenomenon, which occurs frequently in shallow water navigation but has a greater impact on canal passage by using (CFD) method. where the simulation of passing the KCS in Suez Canal is the first part of the work. Its purpose was to learn how to prepare the geometric model, suitable grid generation, setting-up the mathematical model in (CFD) software STAR-CCM+ and compare the results with (EFD) data. The (CFD) simulation is carried out for a range of ship speeds at a H/T ratio of 2.2, the sinkage, trim, and total resistance coefficient data of the KCS are provided. Additionally, the (CFD) results of the ship's hydrodynamics values were compared with those from the available experiments. The general agreement between the (CFD) simulations and experimental tests' predictions of resistance is acceptable. It can be concluded that the performance and ability of STAR-CCM+ could predict free surface flow around a model ship hull and evaluate the ship's hydrodynamics in the Suez Canal accurately.

The other purpose of the present study was to provide information about squat's effects for marine officers in order to avoid any ship accidents when they are sailing in Suez Canal by using trim and sinkage curves which results from this study and this curve would help the officers and give them an assessment on the effects of squat so that they can choose the right speed which gives minimum squat to sail their ship safely in the canal. Future studies would focus on studying the effect of ship draft, hull shapes, dimensional ratios, canal depth and weather conditions in canal on the resistance, trim and squat for a ship sailing in Suez Canal.

9. LIST OF SYMBOLS

ρ	: Fluid density (kg/m^3)
μ	: Dynamic viscosity (Pa.s)
β	: Scale factor (-)
S	: Blockage factor (-)
τ	: Trim angle ($\circ$)
ε	: Turbulence dissipation rate(m^2/s^3)
Δx	: Mesh cell dimension(m)
U_0	: Mesh flow speed
D	: Ship's depth(m)
T	: Ship's draft (m)
LCG	: Longitudinal Distance to Centre of Gravity(m)
KG	: Vertical Centre of Gravity(m)
K	: Turbulent kinetic energy (m^2/s^2)
h	: Water depth (m)
CL	: Centre line
BL	: Base line
B	: Ship's breadth
AP	: Aft perpendicular
A_S	: Wetted area(m^2)
Δt	: Time step (s)

Δy	: Distance between wall and the first knot of the mesh(m)
δ_{max}	: Maximum squat (m)
x_i	: x, y, and z.
$\bar{p}$	: Mean pressure (Pa)
g_i	: Gravity acceleration component (m/s^2)
I	: Turbulence Intensity (-)
R_n	: Reynolds number (-)
C_B	: Block coefficient (-)
C_F	: Friction resistance coefficient (-)
C_R	: Residual resistance coefficient (-)
C_W	: Wave resistance coefficient (-)
C_{VP}	: Viscous pressure resistance coefficient (-)
C_T	: Total resistance coefficient (-)
C_{TM}	: Total model resistance coefficient (-)
F_{rh}	: Froude depth number (-)
R_T	: Total resistance (N)
T_{FP}	: Ship draught at forward perpendiculars (m)
T_{AP}	: Ship draught at aft perpendiculars (m)
$\bar{\tau}_{ij}$	: Stress tensor
TVR	: Turbulent/Viscosity Ratio (-)
LOA	: Length overall (m)
L_{PP}	: Length between perpendiculars (m)
k_{YY}	: Pitch radius of gyration(m)
k_{xx}	: Roll radius of gyration(m)
$\bar{u}_i$	: u, v, w the velocity components of the flow in the (x, y, z) coordinate directions(m/s)
V_K	: Forward speed (m/s)
V_S	: Ship speed (m/s)
V_M	: Model speed (m/s)
μ_t	: Turbulent eddy viscosity (Pa.s)
u_τ	: Friction velocity (m/s)

CREDIT AUTHORSHIP CONTRIBUTION STATEMENT

Osama M. EL-Desouky: Conceptualization, Methodology, Software, Analysis, Writing Review & Editing, Supervision.

Yasser El-henawy: Analysis and Editing.

DECLARATION OF COMPETING INTEREST

The authors declare that they have no known competing financial interests or personal relationships that could have appeared to influence the work reported in this study.

DECLARATION OF FUNDING

10. REFERENCE

[1] H. Duarte, M. Lutzhoft, P.Pereira, "Review of practical aspects of shallow water and bank effects," International Journal of Maritime Engineering (Transactions of the Royal Institution of Naval Architects: Part A), 158 (A3),2016, pp.177-186.
https://DOI No: 10.3940/rina.ijme.2016.a3.362

[2] M. Kazerooni, M.Seif, , "Experimental study of a tanker ship squat in shallow," Jurnal Teknologi (Sciences and Engineering) ; Vol. 66, Issue. 2, 2014, pp. 15-20.
https://https://doi.org/10.11113/jt.v66.2477.

[3] D.Oscar, N.Kazuo, H.Jairo, "Hydrodynamic analysis of inland self-propelled vessel for cargo transportation in the magdalena river," Proceeding of the VI International Ship Design & Naval Engineering Congress (CIDIN) and XXVI Pan-American Congress of Naval Engineering, Maritime Transportation and Port Engineering (COPINAVAL) ,2019, pp. 134-152.
https://doi.org/10.11606/D.3.2019.tde-22082019-142046

[4] T. Tezdogan, M. Terziev, E. Oguz, A. Incecik, "Numerical Analysis of The Behaviour of Vessels Advancing Through Restricted Shallow Waters," Journal of Fluids and Structures, 2018, pp.185-215.
https://DOI:10.1016/j.jfluidstructs.2017.10.003

[5] N. Hoa, V. Bich, T. Tu, "Numerical investigating the effect of water depth on ship resistance using rans cfd method," Polish Maritime Research 3 (103) Vol. 26, 2019.pp. 56-64.
https://DOI:10.2478/pomr-2019-0046

[6] P. ŞERBAN, "Correlation Between a Ship's Geometric and Functional Parameters and Channel Navigation," PhD Thesis, Politehnica University of Bucharest, Faculty of Power Engineering,2017.

[7] Suez Canal Authority, 2018;
http://looklex.com/e.o/suez_can.htm

[8] J.Verwilligen, M.Mansuy, M.Vantorre, "Full-scale measurements to assess squat and vertical motions in exposed shallow water," Proceedings of the 34th PIANC World Congress in Panama City, Panama ,2018, pp. 461–462.

[9] J. Švetak, "Ship squat," Promet-Traffic-Traffico, Vol. 13, No.4,2001, pp.247-251.

[10] K.S. Varyani, "Squat effects on high-speed craft in restricted waterways," Journal of Ocean Engineering ,Volume 33, Issues 3–4 ,2006 , pp. 365-381.

https://doi.org/10.1016/j.oceaneng.2005.04.016

[11 CD-Adapco STAR-CCM+ User's Guide. Version 14.02.010-R8. CD-adapco. 2019.

[12] T.Tezdogan, A. Incecik, O. Turan, "A numerical investigation of the squat and resistance of ships advancing through a canal using cfd," Journal of Marine Science and Technology volume 21, 2015 ,pp. (86–101).
https://DOI:10.1007/s00773-015-0334-1

[13] SIMMAN 2014. Workshop on verification and validation of ship manoeuvring simulation methods. Copenhagen,2014,

https://simman2014.dk.

[14] International Towing Tank Conference (ITTC), Practical guidelines for ship CFD applications, in: Proc. 26th ITTC,2014.

[15] International Towing Tank Conference (ITTC), Recommended Procedures and Guidelines - Uncertainty Analysis in CFD Verification and Validation Methodology and Procedures ,2017.

[16] H. Kazemi, M. Salari, "Effects of loading conditions on hydrodynamics of a hard-chine planing vessel using cfd and a dynamic model," International Journal of Maritime Technology, Vol.7, 2017, PP.11-18.
 https://DOI:10.18869/acadpub.ijmt.7.11

[17] K. Elsherbiny, M. Terziev, T.Tezdogan "Numerical and experimental study on hydrodynamic performance of ships advancing through different canals," Journal of Ocean Engineering, Volume 195, 2019, p.106696.

https://doi.org/10.1016/j.oceaneng.2019.106696